04-82-C3

Corrosion Science, Vol. 22, No. 8, pp. 739–751, 1982
Printed in Great Britain.

0010-938X/82/080739-12 $03.00/0
Pergamon Press Ltd.

PITTING AND PITTING INHIBITION OF IRON IN SODIUM SULPHATE SOLUTIONS†

A. D. KEITELMAN and J. R. GALVELE

Comisión Nacional de Energía Atomica, Departamento Materiales, Av. Libertador 8250, 1429 Buenos Aires, Argentina

Abstract—The anodic behaviour of high purity iron in 0.5 M sodium sulphate solutions was studied. Experiments were made in both acid and alkaline solutions (pH 2.7, pH 9.0, pH 10.0 without buffers; and pH 9.2 with borate buffer). Anodic polarization curves, and surface scratching experiments, showed pitting potentials in 0.5 M Na_2SO_4 pH 9.0 and pH 10.0 solutions. Their values were very close to the corrosion potential obtained in a 0.5 M Na_2SO_4, pH 2.7, pit-like solution. The pitting potential in a borate buffered 0.5 M Na_2SO_4 solution was 50 mV higher than that in the unbuffered solutions. The pitting inhibition potential measured in a 0.5 M Na_2SO_4 solution, pH 10.0, was very close to the passivation potential found in the pit-like solution. All these facts can be explained by the localized acidification mechanism for pitting. The pitting potential is the minimum potential at which an acidified solution can be produced and maintained in contact with the dissolving metal. Similarly the pitting inhibition potential is the electrode potential at which the metal becomes passive in the pit-like solution.

INTRODUCTION

MANY PASSIVE metals, when exposed to the action of aggressive anions, undergo a type of localized corrosion known as pitting. For most metals or alloys a pitting potential (E_p) below which pitting does not occur, was found. This critical potential depends both on the metal or alloy and on the electrolyte composition. Moreover, pitting inhibition potentials (E_i), above which no pitting was observed, were found[1-3] in certain metal solution systems.

From available experimental evidence, localized acidification on the metal–solution interface was proposed[1-6] as a controlling step in the pitting process. According to this, the pitting potential (E_p) is the minimum potential at which such acidification can be maintained at the metal–solution interface. Consequently, E_p must be equal to, or higher than, the corrosion potential (E_c^*) of the metal in the pit-like solution: $E_p \geq E_c^*$. Similarly[6] the pitting inhibition potential (E_i) should be close to the passivation potential (E_{pas}), above which the metal becomes passive in the acid solution; ($E_i \simeq E_{pas}$). In the present work the behaviour of pure iron in sulphate solutions was examined to verify such a mechanism.

Many researchers[2,7-16] have been concerned with the influence of sulphate on the corrosion of iron. Freiman and Kolotyrkin have studied the conditions under which two active–passive transitions occur in this system.[7] They showed that the second transition potential is independent of the pH in the pH range 2–12, both in buffered and non-buffered 0.5 M Na_2SO_4 solutions. Later, Vetter and Strehblow[2] showed that this second passive state was due to a pitting process and they identified the second passivation as the inhibition potential described by Schwenk.[1] They reported $E_i = +480$ mV in 0.5 M Na_2SO_4 pH 4.6, pH 8.0, and pH 9.3 phtalate or borate

†Manuscript received 5 January 1982.

buffer solutions. Gibbs and Cohen,[8] working with 0.15 N Na_2SO_4, pH 8.4, solutions pointed out the influence of both the degree of initial oxidation of the iron surface in air and the polarization time on the shape of the anodic polarization curve. For completely cathodically reduced specimens a breakdown potential at $E = -385$ mV was found. At much higher potentials pits were so numerous that they looked like general attack. Smialowska[9] has examined the nucleation and propagation of pits in 0.5 M Na_2SO_4, pH 7. The potential range where pitting was observed was found to be from -50 to *ca.* $+475$ mV. Prolonged polarization under this potential region produced integration of pits and general corrosion. At higher anodic potentials, passivation was obtained. Finally, Kodama,[10] working with Na_2SO_4 over the concentration range of 10^{-4}–10^{-1} M in borate solutions pH 8.45, found that the pitting potentials became less noble and the pitting current higher, with an increase in sulphate concentration.

Thus, the present paper intends mainly to describe the electrochemical behaviour of iron in 0.5 M Na_2SO_4 solutions at pH 9.0, pH 10.0 and pH 9.2 with borate buffer Because low pH values were reported[17] inside iron pits, and no substantial changes of the electrolyte concentration were expected[4,18] at the initial steps of pit growth, a 0.5 M Na_2SO_4 pH 2.7 was chosen to represent the pit-like solution in the present work.

Pitting potential measurements and pitting inhibition potential measurements obtained by potentiostatic and scratching[19] techniques gave potentials at which pits grew from very small dimensions to visible size. Observations of the samples and the pit morphology were also performed by means of optical microscopy and scanning electron microscopy. Very good agreement was found between E_p–E_i and E_c^*–E_{pa}, respectively, such as predicted by the acidification mechanism.

EXPERIMENTAL METHOD

Apparatus

The measurements were made at 25 ± 0.5°C in a Pyrex glass cell with a platinum counter electrode. Potentials of the samples were measured through a Luggin capillary with a mercurous sulphate reference electrode. All potentials are reported in the normal hydrogen scale (NHE).

Potentials were kept constant with a LYP electronic potentiostat, while they were measured with a LYP electronic millivoltmeter. Currents were recorded with a Tacussel TI 20 G recorder.

Solutions

The anodic behaviour of high purity iron was studied in the following solutions: (i) 0.5 M Na_2SO_4 (pH 2.7; 9.0; and 10.0); (ii) 0.5 M Na_2SO_4 + 0.005 M $Na_2B_4O_7.10\,H_2O$ (pH 9.2). The solutions were prepared with analytical grade reagents and distilled water and were de-aerated with purified nitrogen.[20] Nitrogen was bubbled through the solutions during the tests. The pH of the solutions was adjusted by addition of the corresponding strong acid (H_2SO_4) or base (NaOH), with the exception of the solutions with tetraborate decahydrate, which spontaneously reached pH 9.2.

Iron electrodes

In alkaline solutions 5 mm dia 99.999% iron cylindrical rods from Gallard-Schlesinger (England) were used. By cutting this material, 12 mm long cylinders were obtained. These were pickled with HNO_3 10% (v/v). A copper wire lead was soldered to one of the flat faces of the sample. The electric contact, the unpolished faces, and the edges of the specimens were covered with an epoxy resin cured at 70°C, leaving an exposed free surface of about 0.1 cm^2.

Due to intense dissolution at pH 2.7, to reduce the IR drop, 1 mm dia 99.99% iron wires from Leico Industries (U.S.A.) were used in this medium. The wire was cut to give 12 mm long samples and a copper wire was soldered to one end of them.

The flat surface of the specimens used in alkaline solutions was polished to 1 and 0.3 micron alumina. Wire specimens were abraded with 600 SiC paper and pickled for 2 min in 30% (v/v) HNO_3 at room temperature immediately before the electrochemical test.

Before measurements, the samples were cathodically polarized for 20 min at a constant current density (50 μA cm^{-2}) in order to reduce the initial surface iron oxide.

Procedure

Quasi-stationary potentiostatic polarization curves were obtained in 0.5 M Na_2SO_4 pH 2.7 solutions, by changing the potential in steps of 50 mV, starting from the corrosion potential (−410 ± 10 mV). The current was measured after 5 min at constant potential.

Potentiostatic ascending and descending polarization curves were obtained in 0.5 M Na_2SO_4 pH 9 and 10 solutions, by changing the potential in steps of 50 mV and waiting 10 min at constant potential before measuring the current. Current–time curves, at constant potential, were also obtained in these media, with and without scratching the samples, by switching the potential from an open circuit to the chosen value, and recording the current for at least 120 min. A new specimen was used for each potential. While the samples were kept at constant potential, the surface of the metal was scratched with an SiC point mounted on the Luggin capillary. The change of current with time was then recorded in the same way as in the samples without scratching.

Potentiostatic polarization curves were obtained in 0.5 M Na_2SO_4 + 0.005 M $Na_2B_4O_7.10\ H_2O$ (pH 9.2) solution in steps of 50 mV by scratching the surface of specimens held at constant potential for 10 min. The currents were recorded 10 min after scratching, and then the potential was changed. This procedure was repeated until a potential was reached at which repassivation no longer occurred, current started to increase rapidly and pitting developed on the surface. The ascending polarization curves were initiated at the corrosion potential, *ca.* − 500 mV. The descending polarization curves were initiated at + 1300 mV, 200 mV below the vigorous oxygen evolution zone.

In addition, pits were allowed to grow at constant potential, after scratching the surface of the samples in this medium, and from the size of the pits the mean current density inside the pits was calculated. Measurements of the diameter of the pits were made under a microscope with 100 × magnification. Assuming that the pit grew at a constant rate, the current density inside the pits was calculated with the following equation:

$$\text{Current density } (A\ cm^{-2}) = \frac{r.d.F}{t.E} \qquad (1)$$

where r is the pit radius (in c_m), d is the metal density (in g cm^{-3}), F is the Faraday constant, t is the exposure time (in seconds), and E is the equivalent weight of the metal, assuming that iron dissolves as Fe^{2+}.

EXPERIMENTAL RESULTS

Figure 1 shows the anodic polarization curve of iron in 0.5 M Na_2SO_4, pH 2.7, solution. The corrosion potential was − 410 mV. At potentials from − 410 to + 500 mV rapid dissolution of the specimen was observed with severe attack of the metal surface. From + 500 to + 1500 mV a low current zone was observed with current densities of the order of 10^{-5} Acm^{-2}. At potentials more positive than + 1500 mV oxygen evolution accompanied by severe dissolution and roughening of the metal surface began to be noticeable.

Figure 2 shows a quasi-stationary polarization curve of iron in 0.5 M Na_2SO_4 pH 9. Current densities remained at values of 10^{-4} Acm^{-2} and the specimens presented slight attack. Because the currents plotted in Fig. 2 were not steady values, current–time curves for long time potentiostatic exposures were drawn in order to improve understanding of iron behaviour in this medium. Representative curves were drawn in Fig. 3. Current densities remained at values of 10^{-4}–10^{-3} Acm^{-2} and were not potential-dependent. A great dispersion can be observed for the same potentials, and this behaviour can be related to the superposition of pitting and general dissolution corrosion undergone by the samples. In fact, at potentials lower than about − 390 mV general attack was observed. At potentials higher than this value, both pitting and general dissolution appeared on the specimens.

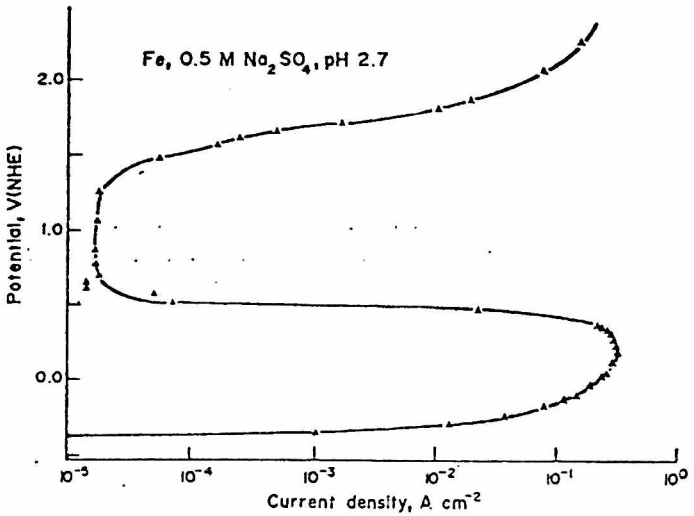

FIG. 1. Anodic quasi-potentiostatic polarization curve of high purity iron in a deaerated 0.5 M Na_2SO_4 solution, pH 2.7, 25°C, measured in ascending steps of 50 mV each.

Owing to the above current–time curve dispersion, pitting generation was metallographically looked for. For similar exposure times different types of attack could be found to accompany pitting. For example, pitting with general dissolution of diverse intensity (Fig. 4), pitting with practically a passive surface (Fig. 5), or pitting with selective dissolution revealing grain boundaries (Fig. 6) could be found. Pits were hexagonal, following crystallographical planes, and changed to hemispherical, after a time. During polarization, a loose green precipitate, which could be completely

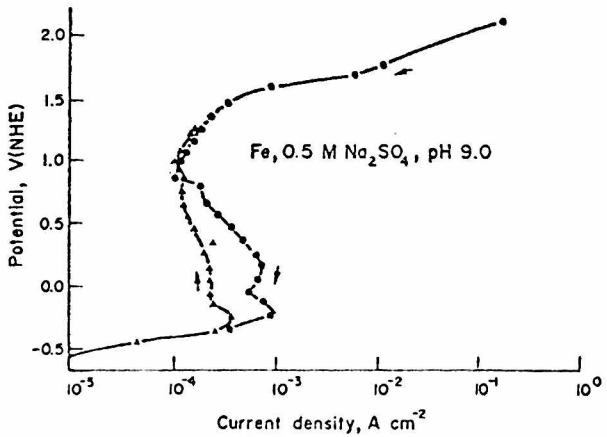

FIG. 2. Anodic quasi-potentiostatic polarization curve of high purity iron in a deaerated 0.5 M Na_2SO_4 solution, pH 9, 25°C, compared measurements of ascending (▲) and descending (●) steps.

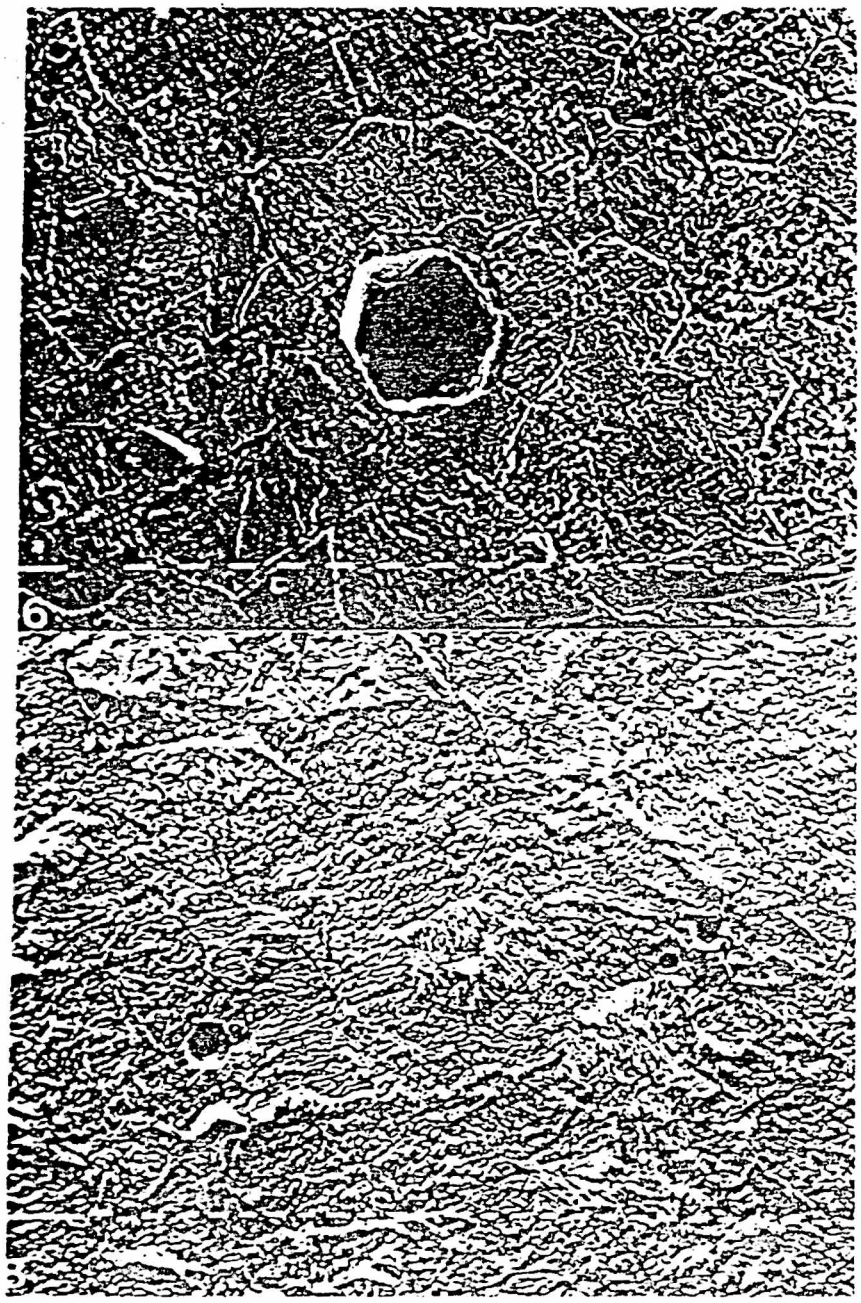

FIG. 6. Scanning electron micrograph of high purity iron exposed to a de-aerated 0.5 M Na_2SO_4 solution, pH 9, 25°C, at − 340 mV for 220 min. Scale = 10 μm. Pitting on an etched surface.

FIG. 8. Scanning electron micrograph of high purity iron exposed to a de-aerated 0.5 M Na_2SO_4 solution, pH 10, 25°C, at − 390 mV for 180 min. Scale = 100 μm. Pitting on a generally corroding surface.

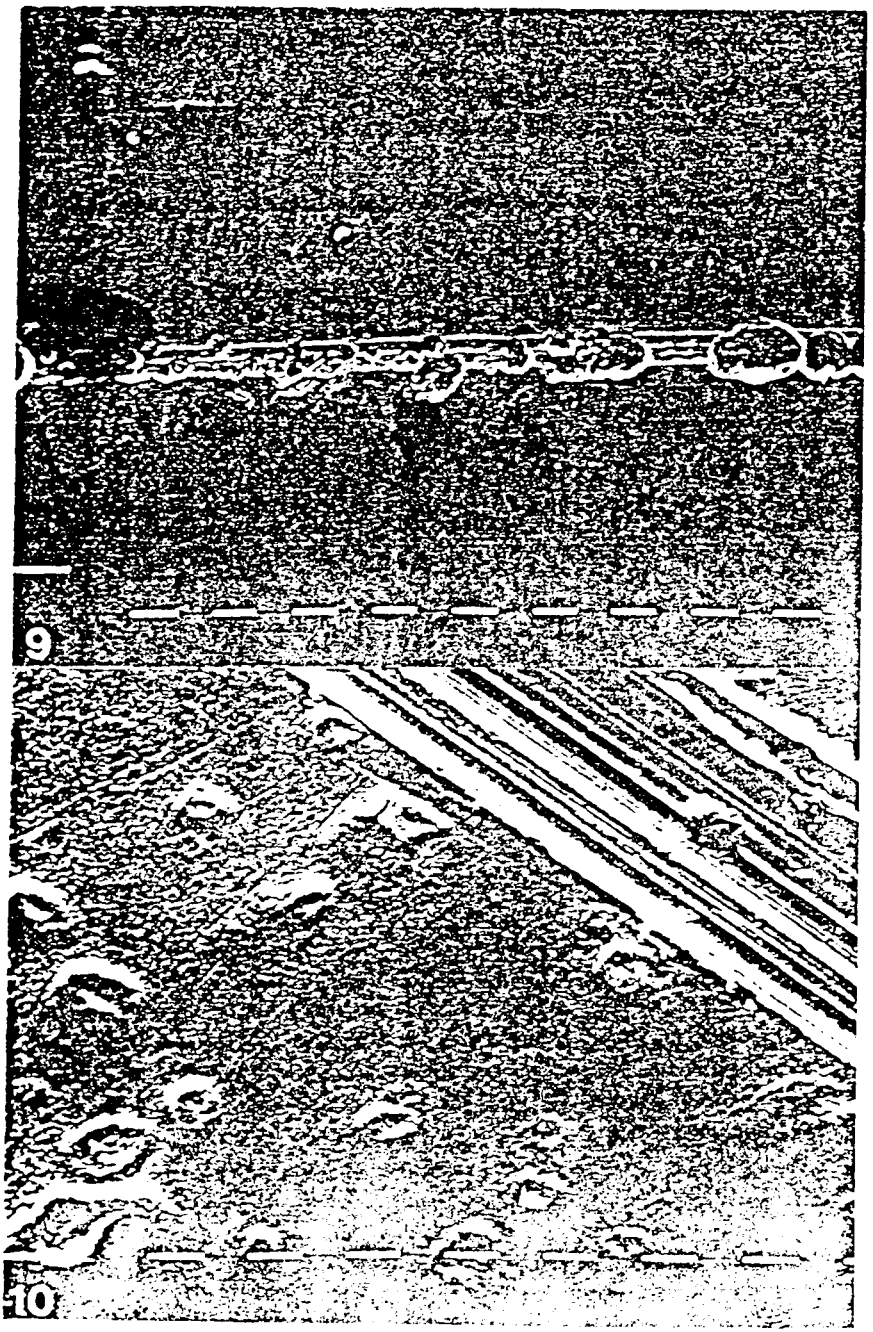

FIG. 9. Pits nucleated along the scratch on a prepassivated specimen of high purity iron, exposed for 40 min after scratching in a de-aerated 0.5 M Na_2SO_4 solution, pH 10, at + 510 mV. Scale = 100 μm.

FIG. 10. Pits nucleated around the scratch on a non-prepassivated specimen of high purity iron, in a de-aerated 0.5 M Na_2SO_4 solution, pH 10, at + 510 mV. Exposure time 40 min. Scale = 10 μm.

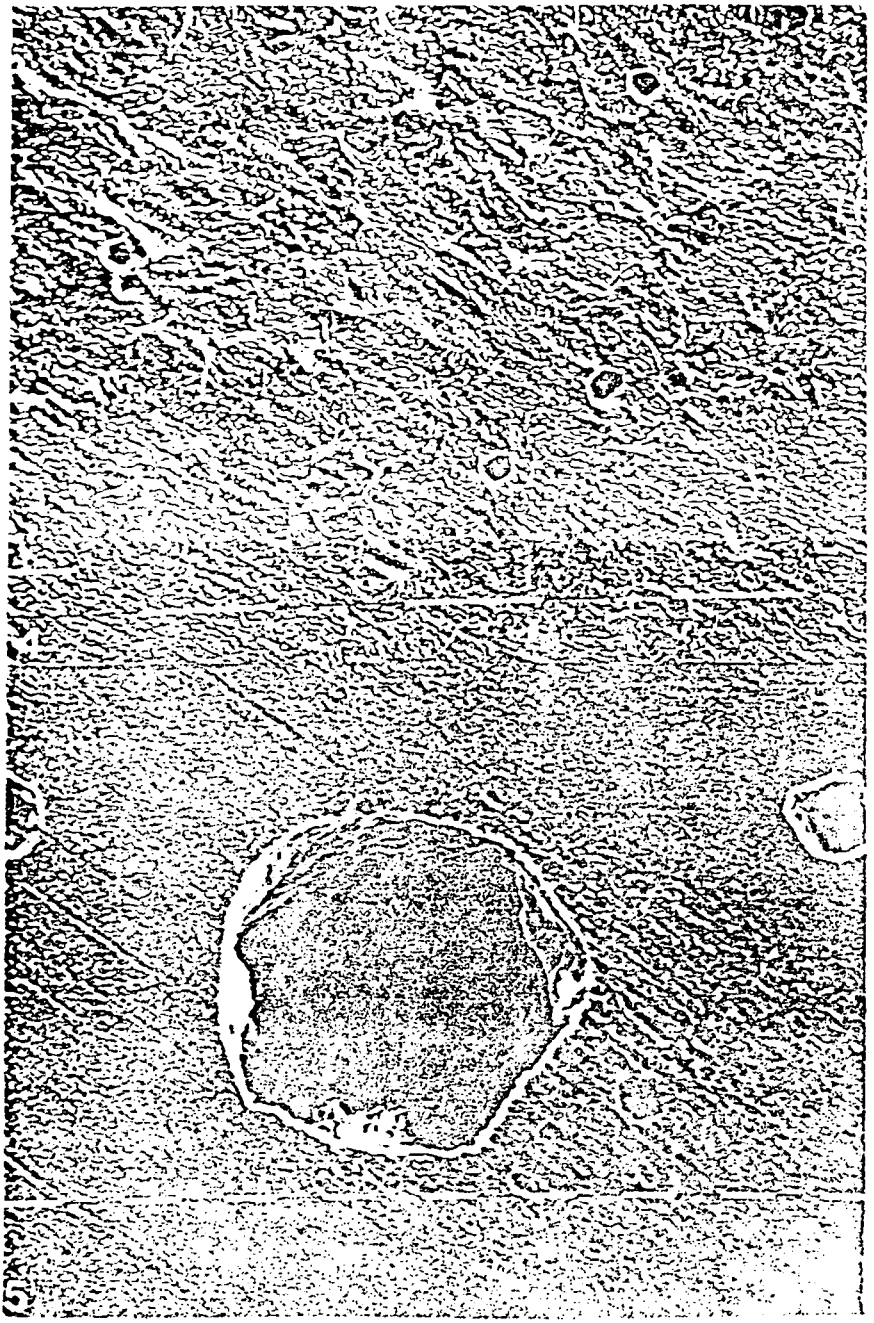

FIG. 4. Scanning electron micrograph of high purity iron exposed to a de aerated 0.5 M Na_2SO_4 solution, pH 9, 25°C, at − 390 mV for 200 min. Scale = 100 μm. Pitting on a generally corroded surface.

FIG. 5. Scanning electron micrograph of high purity iron exposed to a de-aerated 0.5 M Na_2SO_4 solution, pH 9, 25°C, at − 340 mV for 140 min. Scale = 10 μm. Pitting on a passive surface.

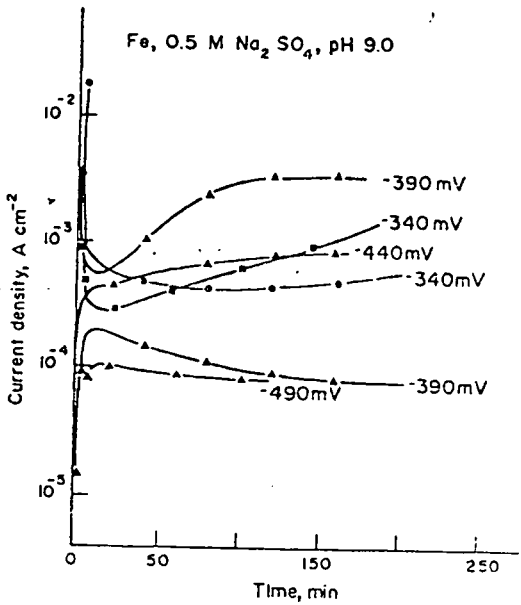

FIG. 3. Typical constant potential current–time curves for high purity iron in a de-aerated 0.5 M Na_2SO_4 solution, pH 9, at 25°C.

removed by washing their surface, covered the samples. In this medium scratching tests did not cause current density significant variations, nor did pitting nucleate on the scratch under such conditions.

To study the pitting process without general attack interference, subsequent runs were carried out at pH 10. The potential range covered (− 540 to + 1200 mV) can be divided into three regions. These are: (I) from corrosion potential ($E_c \cong -540$ mV) up to − 400 mV; (II) from − 400 to *ca.* + 500 mV; (III) from + 500 up to + 1200 mV.

Representative current–time curves for Zones I and II are given in Fig. 7. In Zone I, following an initial transient peak in the first minutes, the current density rapidly decreased to small values, of the order of 1 μAcm^{-2}, remaining constant for times longer than three hours. This was clearly a passive zone and no attack could be observed.

Around − 400 mV a passive to corrosion transition was found. At potentials higher than this value, Zone II, the current density reached a minimum after a few minutes, and then began to increase. Two hours later, the currents reached values of the order of 10^{-4}–10^{-3} Acm^{-2}. In this zone the shape of the current–time curves at − 390 mV and more positive potentials was related to the type of attack. When the current density rapidly reached values of 10^{-3} Acm^{-2}, small pits and intense general attack were observed (Fig. 8). The samples became coated with a spongy green precipitate which could be eliminated by washing, the underlying surface exhibiting severe roughening. On the other hand, when the current density was of the order of 10^{-5} Acm^{-2} during the first minutes and after a minimum increased

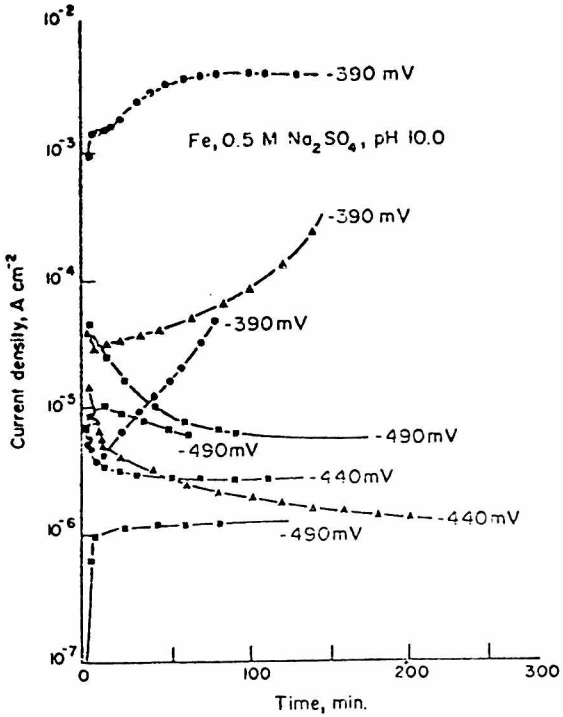

FIG. 7. Typical constant potential current–time curves for high purity iron in a de-aerated 0.5 M Na_2SO_4 solution, pH 10, 25°C.

monotonically to a value of 10^{-4} Acm^{-2} in two hours, pitting attack took place while the rest of the surface remained passive. By allowing a film to grow in the passive Zone I for 90 min and then switching the potential to Zone II, only pitting was obtained remaining the rest of the surface passive.

At about + 500 mV the transition to Zone III was produced. This region presented current densities of the order of 10^{-6}–10^{-5} Acm^{-2}. However, current peaks up to one order of magnitude higher than the "base" current appeared at intervals varying from 30 s to 10 min. The surface of the specimens remained passive, but severe attack on the borders, with crevice corrosion, was found. The appearance of this attack caused a great dispersion in the recorded current–time curves. Nevertheless, the microscopic observation of the samples showed that, except for crevice corrosion, the surface of the samples remained passive.

Scratching experiments

After growing a film at − 490 mV for 90 min, the surface scratching technique was employed at pH 10. The ascending polarization curve thus obtained showed a passive zone where the current density was lower than 10^{-5} Acm^{-2}, and a breakdown potential above which high current increases and passivity breakdown were observed.

The breakdown potential thus obtained was -380 ± 10 mV. Above this potential small pits developed out of the scratch on the surface.

The descending polarization curves were also obtained through the scratching technique with prepassivated samples as described before. The runs were carried out starting from + 1200 mV, and the current densities fluctuated in the order of 10^{-6}–10^{-5} Acm^{-2} with frequent oscillations. The borders of the samples underwent intense attack, just as pointed out in the case of the current time tests. When potentials equal to, or lower than, + 510 mV were applied, the currents after scratching reached values one order of magnitude above those in the higher potential region. Under such conditions pits nucleated on the scratch (Fig. 9). They began by being crystallographic but soon evolved to hemispherical brightened pits. If the specimens were not prepassivated, pits, plugged up with corrosion products, were found around the scratch (Fig. 10). The scratched zone and its surroundings showed a brown precipitate in contrast to the green precipitate observed at lower potentials.

Anodic behaviour of iron in sulphate plus borate solutions

Figure 11 shows the ascending and descending polarization curves performed in 0.5 M Na_2SO_4 + 0.005 M $Na_2B_4O_7.10\ H_2O$ (pH 9.2) by scratching the samples.

As the potential was increased above the corrosion potential (*ca.* — 520 mV), the current density also increased to small values, of the order of 1 μAcm^{-2}, reaching a peak of 5.6 μAcm^{-2} around — 450 mV. In spite of an active loop appearance, the samples remained passive in this region, occasionally showing some slight attack on the borders. Above — 450 mV the current density began to decrease. At — 350 mV the current density reached a minimum value, and there was an abrupt increase of two orders of magnitude at higher potentials.

Current densities, that did not vary significantly with time after scratching, were found between the corrosion potential and — 350 mV. After scratching the surface

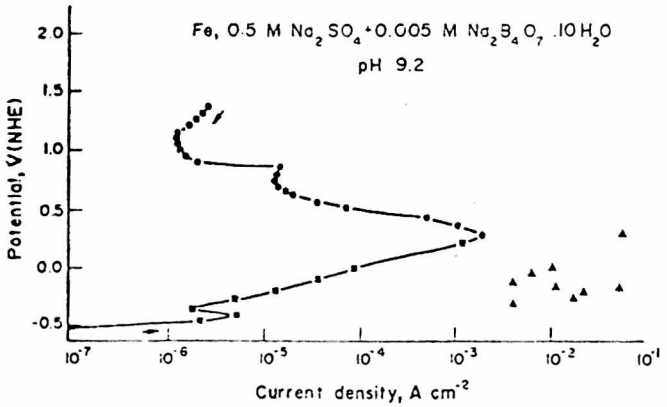

Fig. 11. Anodic potentiostatic polarization curves of high purity iron in de-aerated 0.5 M Na_2SO_4 + 0.005 M $Na_2B_4O_7$, pH 9.2, at 25°C, obtained with the scratch technique ■: ascending steps measurements; ●: descending steps measurements; ▲: current density values, inside the pits, calculated with Equation (1).

at these potentials the current increased but almost immediately returned to the initial value. For higher potentials, on the other hand, the current density increased after scratching and continued to increase with time in this region.

All the samples exposed at potentials higher than − 350 mV pitted and the measured current densities mainly corresponded to pit growth. Pits were observed on the centre and the borders of the specimens rather than along the scratch.

Descending anodic polarization curves were obtained starting from + 1300 mV (Fig. 11). The curve showed a passive zone, up to + 860 mV, with current densities of about 1 μm Acm^{-2}. In this region the stationary current density was not affected by scratching the metal surface.

When potentials from + 860 to + 500 mV were applied, the current did not decay after scratching, but reached values one order of magnitude above those of the upper passive zone. From + 500 mV to + 350 mV the current density also increased and reached values of the order of 10^{-3} Acm^{-2}. There was severe attack on the borders all over the high potential region, from + 1300 to + 350 mV. These results pointed out that curves like those in Fig. 11 are real polarization curves with true current densities only at potential ranges where localized corrosion could not be observed (between the corrosion potential and − 350 mV, and from + 1300 to + 860 mV).

To overcome this difficulty and establish the pitting zone, constant potential experiments were performed by scratching the samples at potentials from −350 to + 860 mV. After the current started to increase specimens were kept at constant potentials for approx. 90 to 240 min to allow pits to grow. Then they were removed from the cell and the mean radius of the pits was measured under the microscope. The current density inside the pits was calculated through equation (1).

Pitting was nucleated only between − 350 and + 350 mV. The pits grown in this region showed repassivation when the potential was switched to about + 500 mV, and their current density decreased from 10^{-3} to 10^{-5} Acm^{-2}. Figure 11 shows the calculated current density values inside the pits. The diameter of the pits varied between 0.03 and 0.2 mm, and the calculated current density values ranged from 4×10^{-3} up to 6×10^{-2} Acm^{-2}. The value found near the pitting potential was 4×10^{-3} Acm^{-2}.

DISCUSSION AND CONCLUSIONS

Anodic polarization curves, current–time curves, surface scratching experiments and metallographic observations in various alkaline Na_2SO_4 solutions indicated that iron undergoes pitting in the presence of these electrolytes. The pitting potential measured in 0.5 M Na_2SO_4 solution, pH 9.0 and 10.0, was − 400 mV, while the value in 0.5 M Na_2SO_4 + 0.005 M $B_4O_7Na_2$ pH 9.2 solution was − 350 mV. These values were close to the corrosion potential obtained for iron in the 0.5 M Na_2SO_4, pH 2.7, pit-like solution (E_c = − 410 mV). According to the mechanism of localized acidification[4-6] the pitting potential of a metal or alloy in a neutral or alkaline solution can be evaluated from the anodic behaviour of the same metal or alloy in a low pH pit-like solution. The pitting potential in the neutral or alkaline solution is given by

$$E_p = E_c^* + \eta + \varphi + E_{inh} \qquad (2)$$

where E_p is the pitting potential, E_c^* is the corrosion potential in the acidified solution,

η is the polarization necessary to obtain a current density high enough to maintain acidity inside the pit, φ is the potential drop inside the pit and E_{inh} is the contribution to the polarization due to inhibitors in the medium.

In 0.5 M Na_2SO_4, pH 2.7, solutions (see Fig. 1) high current densities are obtained with small polarization. Therefore the contribution of η to the pitting potential is small. The same happens with φ, since the current density inside the pits (see Fig. 11) near the pitting potential was relatively low, 4.10^{-3} Acm^{-2}, and a high concentration electrolyte was used. On the other hand, the pitting potential in a buffered 0.5 M Na_2SO_4 solution (0.005 M $Na_2B_4O_7$, pH 9.2) was 50 mV above that in unbuffered solutions. This difference must be attributed to the presence of the buffer (E_{inh}).

The pitting inhibition potentials measured in 0.5 M Na_2SO_4, pH 10, and 0.5 M Na_2SO_4 + 0.005 M $Na_2B_4O_7$, pH 9.2, were *ca.* + 500 mV in both cases. Due to general attack no pitting inhibition potential could be established in 0.5 M Na_2SO_4, pH 9. Those values are a little higher than the inhibition potentials found by Vetter and Strehblow[2] in sulphate solutions with higher buffer concentrations and by Szklarska-Smialowska[9] in 0.5 M Na_2SO_4, pH 7. All these results compare very well with the passivation potential, E_{pas} = + 500 mV, obtained in the 0.5 M Na_2SO_4, pH 2.7, pit-like solution. This fact was also explained by the acidification mechanism.[5] For iron in Na_2SO_4 solutions, when the electrode potential reaches the value of passivation of the metal in the acid solution, the metal inside the pit will become passive and pitting will stop. Then the pitting inhibition potential is essentially the passivation potential of the metal in the acidified pit-like solution. In the systems studied in the present work the inhibition potential, E_i, seems to have scarce practical use due to crevice corrosion. Apparently in those regions where a high potential drop can be found, like in a crevice, the inhibition potential is not reached, and localized corrosion can proceed.

Acknowledgements—This research has been supported by the Comisión de Investigaciones Cientificas de la Provincia de Buenos Aires (C.I.C.), by the Servicio Naval de Investigación y Desarrollo, Programa ECOMAR and by the Proyecto Multinacional de Tecnologia de Materiales, OEA-CNEA.

REFERENCES

1. W. Schenk, *Corrosion* 20, 129t (1964).
2. K. J. Vetter and H. H. Strehblow, *Ber. Bunsenges. physik. Chem.* 74, 449 (1970).
3. H. H. Strehblow and B. Titze, *Corros. Sci.* 17, 461 (1977).
4. J. R. Galvele, *J. electrochem. Soc.* 123, 464 (1976).
5. J. R. Galvele, in *Passivity and its Breakdown on Iron and Iron Base Alloys*, (edited by R. W. Staehle and H. Okada), p. 118. NACE, Houston (1976).
6. J. R. Galvele, in *Passitivty of Metals* (edited by R. P. Frankenthal and J. Kruger), p. 285. The Electrochem. Soc., Princeton (1978).
7. L. I. Freiman and Ya. M. Kolotyrkin, *Dokl. Akad. Nauk. USSR* 171, 1138 (1966).
8. D. B. Gibbs and M. Cohen, *J. electrochem. Soc.* 119, 416 (1972).
9. S. Szklarska-Smialowska, *Corros. Sci.* 18, 97 (1978).
10. T. Kodama, in *Proc. Fifth Int. Cong. Metallic Corros.*, p. 223. NACE, Houston (1975).
11. J. Tousek, *Corros. Sci.* 12, 15 (1972).
12. S. Szklarska-Smialowska and G. Mrowczynski, *Br. Corros. J.* 10, 187 (1975).
13. S. Szklarska-Smialowska, *Br. Corros. J.* 10, 192 (1975).
14. D. Geana, A. A. El Miligy and W. J. Lorenz, *Corros. Sci.* 13, 505 (1973).
15. D. Geana, A. A. El Miligy and W. J. Lorenz, *J. appl. Electrochem.* 4, 337 (1974).
16. J. V. Dobson, T. Dickinson and P. R. Snodin, *J. electroanal. Chem.* 88, 363 (1978).
17. J. A. Smith, M. H. Peterson and B. F. Brown, *Corrosion* 26, 539 (1970).
18. K. J. Vetter and H. H. Strehblow, *Ber. Bunsenges. physik. Chem.* 74, 1024 (1970).
19. N. Pessall and C. Liu, *Electrochim. Acta* 16, 1987 (1971).
20. D. Gilroy and J. E. O. Mayne, *J. appl. Chem.* 12, 382 (1962).